

$h \rightarrow \gamma\gamma$ and $h \rightarrow Z\gamma$ in the Inert Doublet Higgs Model and type II seesaw Model

Abdesslam Arhrib

Université AbdelMalek Essaadi, Faculté des sciences et techniques, B.P 416 Tangier, Morocco

In this talk we discuss the rate of $h \rightarrow \gamma\gamma$ and $h \rightarrow Z\gamma$ in the Inert Higgs Doublet Model and the type II seesaw model. In the the Inert Higgs Doublet the 2 channels are correlated. In the type II seesaw model it is found that $h \rightarrow \gamma\gamma$ and $h \rightarrow Z\gamma$ can be correlated or anti-correlated.

I. INTRODUCTION

The first phase of LHC run at 7+8 TeV has been very successful, and confirmed once more the success of the Standard Model (SM). Both experiments ATLAS and CMS at LHC reported discovery of a Higgs-like particle with a mass in the range 125-126 GeV [1], [2]. The new observed Higgs-like state have properties consistent with the SM Higgs boson. More data from the second phase run of LHC at 13 TeV is needed in order to fully pin down the nature of this new state.

The precision measurements, achieved up to now at LHC, of the Higgs-like couplings to fermions and gauge bosons tells us that this Higgs-like particle behaves more and more SM-like. Hence, its properties should be studied as precisely as possible in order to detect any deviation from SM predictions which may reveal presence of new physics. Such measurements, if accurate enough, can be also helpful in discriminating between models through their sensitivity to radiative correction effects, in particular in specific cases like the decoupling limit. It is well known that many SM extensions (like SM with extended Higgs sector, Supersymmetric models, ...) possess such decoupling limit where the light Higgs boson completely mimic the SM Higgs.

Although, CMS and ATLAS data shows no large deviation of the signal from the SM predictions, at ATLAS the diphoton channel shows some small enhancement. The overall signal strength for diphoton is about $1.65 \pm 0.24(stat)_{-0.18}^{+0.25}(syst)$, (which include gluon gluon fusion, vector boson fusion as well as Higgs-strahlung production mode) corresponds to 2.3σ deviation from the SM prediction [3]. Note also that all those individual channels show a bit more than 2σ deviation. However, at CMS, the new analysis for diphoton channel [4] shows different result from the previous one [2]. CMS uses 2 different methods for this channel and get the following results: $0.78_{-0.26}^{+0.28}$ and $1.11_{-0.30}^{+0.32}$ which are compatible within $1.5\text{-}\sigma$ [4]. Combining the above three results will give a signal strength of 1.18 ± 0.16 .

Same as for the diphoton signal, $h \rightarrow \gamma Z$ is also a clean finale state to search for at LHC. This decay can also provide some complementary informations on the Higgs properties such as the mass, parity and spin. In both $h \rightarrow \gamma\gamma$ and $h \rightarrow \gamma Z$ cases, one have the same charged particles contributing to both of them. Although the kinematics and the Z couplings to the charged particles may be slightly different, those 2 channels $h \rightarrow \gamma\gamma$ and $h \rightarrow \gamma Z$ should be correlated to some extent. Moreover, with diphoton channel is now measured by ATLAS and CMS, one could deduce some typical range for $h \rightarrow \gamma Z$. Recently both ATLAS and CMS publish their experimental searches for $h \rightarrow \gamma Z$, the upper limit on the cross section times Branching ratio normalized to SM rate is about 10 (for CMS) and 19 (for ATLAS) [5].

After ATLAS and CMS announcement of possible excess in diphoton channel, many recent studies addressed such enhancement in various models such as SUSY, extended Higgs sector (like inert Higgs and triplet Higgs models) [6–14]. There is also few works which study the decay $h \rightarrow \gamma Z$ and its correlation with $h \rightarrow \gamma\gamma$ [15–19]. In this talk, we would like to discuss the rate of $h \rightarrow \gamma\gamma$ in the Inert Higgs Doublet Model (IHDM) and in the type II seesaw triplet Higgs model and also study its correlation with $h \rightarrow Z\gamma$ in those two models.

II. INERT HIGGS DOUBLET MODEL

The Inert Higgs Doublet Model (IHDM) [20] is an extension of the Higgs sector of SM which could explain dark matter. The model has an additional Higgs doublet H_2 in addition to the SM Higgs doublet H_1 . Moreover, there is a Z_2 symmetry under which all the SM fields and H_1 are even while $H_2 \rightarrow -H_2$ under Z_2 . We further assume that Z_2 symmetry is not spontaneously broken *i.e.* H_2 field does not develop vacuum expectation value (vev). These doublets in terms of physical fields can be parameterized as:

$$H_1 = \begin{pmatrix} G^+ \\ v/\sqrt{2} + (h + iG^0)/\sqrt{2} \end{pmatrix}, \quad H_2 = \begin{pmatrix} H^+ \\ (S + iA)/\sqrt{2} \end{pmatrix} \quad (1)$$

With G^\pm and G^0 are the Goldstone bosons. The Z_2 symmetry naturally imposes the flavor conservation. The

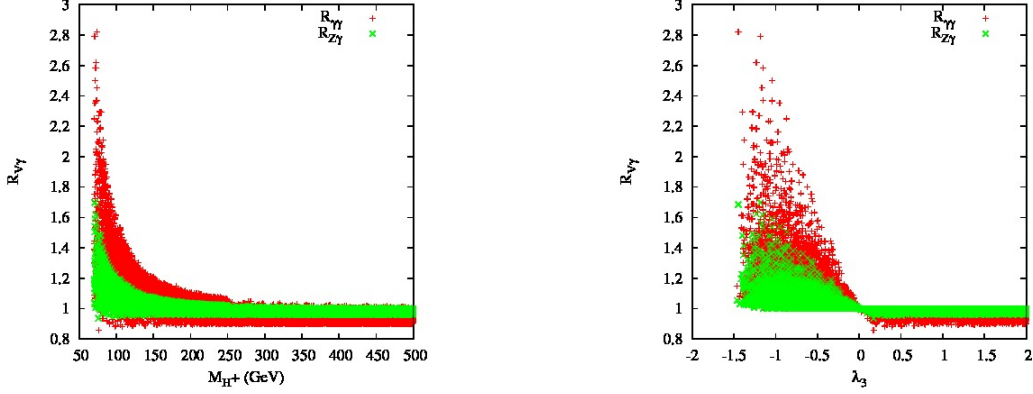


FIG. 1: Signal strength $R_{V\gamma}$ as a function of m_{H^\pm} (left) and as a function of λ_3 (right). With $m_h = 126$ GeV, $m_S \geq 65$ GeV (such that $h \rightarrow SS$ is not open), the other parameters are in this range: $80 < m_{H^\pm, A} < 500$ GeV, $-10^6 < \mu_2^2 < 10^6$ GeV and $-10 < \lambda_2 < 10$.

scalar potential allowed by Z_2 symmetry can be written as:

$$V = \mu_1^2 |H_1|^2 + \mu_2^2 |H_2|^2 + \lambda_1 |H_1|^4 + \lambda_2 |H_2|^4 + \lambda_3 |H_1|^2 |H_2|^2 + \lambda_4 |H_1^\dagger H_2|^2 + \frac{\lambda_5}{2} \left\{ (H_1^\dagger H_2)^2 + h.c. \right\} \quad (2)$$

After electroweak symmetry breaking, the spectrum contains two CP even neutral scalars (h , S) one CP odd neutral scalar (A) in addition to a pair of charged scalars (H^\pm). There is no mixing between the two doublets and hence h plays the role of the SM Higgs Boson. The remaining Higgs Bosons namely S , A and H^\pm are “inert” and they do not have any interaction with quarks and leptons. The Z_2 symmetry also ensures the stability of the lightest scalar (S or A) that can act as a dark matter candidate.

The masses of all these six scalars can be written in terms of six parameters namely: $\{\mu_2^2, \lambda_1, \lambda_2, \lambda_3, \lambda_4, \lambda_5\}$. However, in our study we will use the four physical masses of the Higgs Bosons as well as λ_2 and μ_2^2 as input parameters. The complete set is: $\{m_h, m_S, m_A, m_{H^\pm}, \lambda_2, \mu_2^2\}$ which can be related to the previous parameter set as :

$$\lambda_1 = \frac{m_h^2}{2v^2} \quad , \quad \lambda_3 = \frac{2}{v^2} (m_{H^\pm}^2 - \mu_2^2) \quad , \quad \lambda_4 = \frac{(m_S^2 + m_A^2 - 2m_{H^\pm}^2)}{v^2} \quad , \quad \lambda_5 = \frac{(m_S^2 - m_A^2)}{v^2} \quad (3)$$

III. $h \rightarrow \gamma\gamma$ AND $h \rightarrow Z\gamma$ IN IHDM

In the IHDM, the partial width of $h \rightarrow \gamma\gamma$ and $h \rightarrow Z\gamma$ receives an additional contribution from the charged Higgs boson loops. The partial decay width of $h \rightarrow \gamma\gamma$ can be found in [6] while for $h \rightarrow Z\gamma$ it is given by:

$$\begin{aligned} \Gamma(h \rightarrow Z\gamma) = & \frac{G_F^2 m_W^2 s_W^2 \alpha m_h^3}{64 \pi^4} \left(1 - \frac{m_Z^2}{m_h^2}\right)^3 \left| -2 \frac{3 - 8s_W^2}{3s_W c_W} (I_1(\tau_t, \lambda_t) - I_2(\tau_t, \lambda_t)) \right. \\ & - \cot_w (4(3 - \tan_w^2) I_2(\tau_w, \lambda_w) + ((1 + \frac{2}{c_W}) \tan_W^2 - (5 + \frac{2}{c_W})) I_1(\tau_w, \lambda_w)) \\ & \left. + \frac{1 - 2s_W^2}{s_W c_W} \frac{m_{H^\pm}^2 - \mu_2^2}{m_{H^\pm}^2} I_1(\tau_H, \lambda_H) \right|^2 \end{aligned} \quad (4)$$

where $\tau_i = 4m_i^2/m_h^2$ and $\lambda_i = 4m_i^2/m_Z^2$, ($i = t, W, H^\pm$). The functions I_1 and I_2 can be found in [21]. We stress here that in the SM, as well known, the decay width of $h \rightarrow Z\gamma$ (like $h \rightarrow \gamma\gamma$) is dominated by the W loops which can also interfere destructively with the subdominant top contribution.

In the last term of eq. (4), we have used the coupling of the SM Higgs to a pair of H^\pm which is given by:

$$g_{hH^\pm H^\mp} = -2 \frac{m_W s_W}{e} \lambda_3 = \frac{e(m_{H^\pm}^2 - \mu_2^2)}{2m_W s_W} \quad (5)$$

It is clear from the above Eq. (5), the coupling $g_{hH^\pm H^\mp}$ is completely fixed by λ_3 parameter. Like in the case of $h \rightarrow \gamma\gamma$ [6], for negative (resp positive) λ_3 , H^\pm contributions enhance (resp suppress) both $h \rightarrow \gamma\gamma$ and $h \rightarrow Z\gamma$ rates [6].

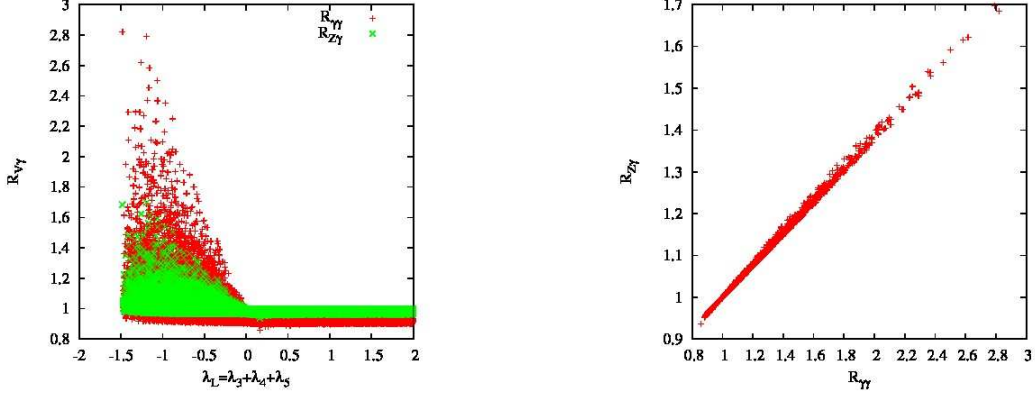


FIG. 2: Signal strength $R_{V\gamma}$ as a function of $\lambda_L = \lambda_3 + \lambda_4 + \lambda_5$ (left) and the correlation between $R_{\gamma\gamma}$ and $R_{Z\gamma}$ (right). Parameters are like in Fig. 1.

The largest contribution to the production cross-section of the Higgs is through gluon fusion. For the higgs decay to $\gamma\gamma$ or γZ channels, we will define the ratio of cross section times branching ratio normalized to the SM one as:

$$R_{V\gamma} = \frac{\sigma(gg \rightarrow V\gamma)}{\sigma(gg \rightarrow V\gamma)^{SM}} = \frac{\sigma(gg \rightarrow h) \times Br(h \rightarrow V\gamma)}{\sigma(gg \rightarrow h)^{SM} \times Br(h \rightarrow V\gamma)^{SM}} \quad , \quad V = \gamma, Z \quad (6)$$

Where we have used the narrow width approximation.

In the IHDM, the Higgs h have the same couplings to fermions as in SM, so the gluon fusion cross section in IHDM is the same as in the SM. Then, eq. (6) will reduce to the ratio of branching ratios. Note also that if the invisible decay $h \rightarrow SS$ is not open, the total width of the Higgs will be approximately the same in both SM and IHDM and in such case eq. (6) will reduce to the ratio of the partial width of $h \rightarrow V\gamma$, $V = \gamma, Z$.

A systematic scan is performed over all the allowed parameter space for $\{m_S, m_A, m_{H^\pm}, \lambda_2, \mu_2^2\}$ with $m_h = 125$ GeV taking into account all the theoretical and electroweak precision constraints described in [6], [7]. In the following scan we will illustrate, the invisible decay of the Higgs will be close since we take $m_S > m_h/2$, such invisible decay if open will only suppress the diphoton and $h \rightarrow Z\gamma$ rates.

Results of our scans are depicted in Fig. 1 and Fig. 2, where we plot both $R_{\gamma\gamma}$ and $R_{Z\gamma}$ as a function of m_{H^\pm} in Fig. 1(left) and as a function of λ_3 in Fig. 1(right). While, in Fig. (2) we plot $R_{\gamma\gamma}$ and $R_{Z\gamma}$ as a function of $\lambda_L = \lambda_3 + \lambda_4 + \lambda_5$ in Figs. 2(left) and we illustrate the correlation between $R_{\gamma\gamma}$ and $R_{Z\gamma}$ in Figs. (2) (right). From those plots, it is clear that enhancing substantially $R_{\gamma\gamma}$ and $R_{Z\gamma}$ we need rather light charged Higgs and negative λ_3 . The enhancement in $h \rightarrow Z\gamma$ is all the time smaller than the one in $h \rightarrow \gamma\gamma$ because the coupling $Z^\mu H^\pm H^\mp = e(1 - 2s_W^2)/(2s_W c_W) \approx 0.67\gamma^\mu H^\pm H^\mp$. The suppression factor of $R_{Z\gamma}$ versus $R_{\gamma\gamma}$ is about 0.67. The lightest is the charged Higgs, the more spectacular are the enhancement of the diphoton and $Z\gamma$. For example, if we need $R_{\gamma\gamma} \geq 1.1$ (resp $R_{Z\gamma} \geq 1.1$) then the charged Higgs has to be lighter than $m_{H^\pm} < 200$ GeV (resp $m_{H^\pm} \leq 115$ GeV) and $\lambda_3 < 0$ (which is $\mu_2^2 > m_{H^\pm}^2$).

In addition, $\lambda_L = \lambda_3 + \lambda_4 + \lambda_5$ is an important parameter which enters in the calculation of the WMIP relic density. This parameter λ_L is constrained from WMAP data to be in the range $|\lambda_L| < 0.2$. We show in Fig. (2)(left) $R_{V\gamma}$ as a function of $\lambda_L \in [-2, 2]$. It is clear that if λ_L is in this range $[-0.2, 0.2]$ allowed by WMAP data, we can still have some enhancement in $R_{\gamma\gamma}$ and $R_{Z\gamma}$.

The correlation between $R_{\gamma\gamma}$ and $R_{Z\gamma}$ is a linear one in this case Fig. (2) (right). As it can be seen from the plot, for $R_{\gamma\gamma} > 1$ where W and H^\pm loops are constructive we have $R_{\gamma\gamma} \geq R_{Z\gamma}$. In the opposite case $R_{\gamma\gamma} < 1$, where W and H^\pm loops are destructive we can have $R_{\gamma\gamma}$ smaller than $R_{Z\gamma}$. The reason is that the

destructive interference between W and H^\pm is acting more on $R_{\gamma\gamma}$ than on $R_{Z\gamma}$ which have much more larger W contribution.

Note that once the invisible decay of the Higgs $h \rightarrow SS$ is open, the branching ratio of $Br(h \rightarrow SS)$ will be the dominant one over all other SM channels unless if one tune the coupling $hSS = \propto m_S^2 - \mu_2^2$ by taking $m_S^2 \approx \mu_2^2$. The opening of the invisible decay $h \rightarrow SS$ would enhance the total width of the SM Higgs boson and therefore suppress both $h \rightarrow \gamma\gamma$ and $h \rightarrow Z\gamma$ branching ratios.

At the end, we would like to comment about $h \rightarrow \gamma\gamma$ and $h \rightarrow Z\gamma$ in the decoupling limit of the general two Higgs doublet Model (2HDM) [24, 25]. In this limit, the SM-Higgs coupling to fermions and to gauge bosons reduces to their SM values. Therefore, only the charged Higgs contributions will modify the rates of $h \rightarrow \gamma\gamma$ and $h \rightarrow Z\gamma$ exactly like in the IHDM. We have shown in [24] that the effect of the charged Higgs on $R_{\gamma\gamma}$ could be on the range $0.75 \leq R_{\gamma\gamma} \leq 1.25$ for $m_{H^\pm} \geq 300$ GeV. The values $R_{\gamma\gamma} \approx 1.2 - 1.25$ and $0.75 - 0.8$ are obtained for m_{H^\pm} close to 300 GeV [24]. The enhancement (resp suppression) happens when the H^\pm contributions are constructive (resp destructive) with the W one.

IV. HIGGS TRIPLET MODEL

Seesaw mechanism for generating small neutrino masses can be achieved without right-handed neutrinos through an extended Higgs sector with $SU(2)_L$ triplet scalar field [26]. The scalar sector of the SM extended by Higgs triplet, which we call Higgs Triplet Model (HTM), consists of the standard Higgs weak doublet H and a colorless scalar field Δ transforming as a triplet under the $SU(2)_L$ with hypercharge $Y_\Delta = 2$, so that $H \sim (1, 2, 1)$ and $\Delta \sim (1, 3, 2)$ under the $SU(3)_c \times SU(2)_L \times U(1)_Y$. Following ref. [22], the general renormalizable and gauge invariant Lagrangian of this scalar sector is:

$$\mathcal{L} = (D_\mu H)^\dagger (D^\mu H) + Tr(D_\mu \Delta)^\dagger (D^\mu \Delta) - V(H, \Delta) + \mathcal{L}_{\text{Yukawa}} \quad (7)$$

where the covariant derivatives are defined by

$$D_\mu H = \partial_\mu H + ig \frac{\sigma^a}{2} W_\mu^a H + i \frac{g'}{2} B_\mu H \quad , \quad D_\mu \Delta = \partial_\mu \Delta + ig \left[\frac{\sigma^a}{2} W_\mu^a, \Delta \right] + ig' \frac{Y_\Delta}{2} B_\mu \Delta \quad (8)$$

W_μ^a and B_μ denoting respectively the $SU(2)_L$ and $U(1)_Y$ gauge fields and σ^a ($a = 1, 2, 3$) the Pauli matrices. The scalar potential $V(H, \Delta)$ is given by,

$$\begin{aligned} V(H, \Delta) = & -m_H^2 H^\dagger H + \frac{\lambda}{4} (H^\dagger H)^2 + M_\Delta^2 Tr(\Delta^\dagger \Delta) + [\mu (H^T i \sigma^2 \Delta^\dagger H) + \text{h.c.}] \\ & + \lambda_1 (H^\dagger H) Tr(\Delta^\dagger \Delta) + \lambda_2 (Tr \Delta^\dagger \Delta)^2 + \lambda_3 Tr(\Delta^\dagger \Delta)^2 + \lambda_4 H^\dagger \Delta \Delta^\dagger H \end{aligned} \quad (9)$$

where Tr is the trace over 2×2 matrices. We write the two Higgs multiplets in components as (the 2×2 traceless matrix representation for the triple is used):

$$\Delta = \begin{pmatrix} \delta^+/\sqrt{2} & \delta^{++} \\ \delta^0 & -\delta^+/\sqrt{2} \end{pmatrix} \quad \text{and} \quad H = \begin{pmatrix} \phi^+ \\ \phi^0 \end{pmatrix} \quad (10)$$

After electroweak symmetry breaking, the spectrum of the HTM contains: 2 neutral CP-even Higgs h and H , one neutral CP-odd Higgs A , a pair of singly charged Higgs H^\pm and a pair of doubly charged Higgs $H^{\pm\pm}$. The doubly charged Higgs state $H^{\pm\pm}$ is pure triplet while the other scalar states h , H , A and H^\pm are mixture of doublet and triplet components. For A and H^\pm Higgs, the mixing between doublet and triplet is very small since it is given by the ratio $v_t/v_d \ll 1$ since the triplet vev v_t is constrained to be of the order of few GeV from electroweak precision measurements. In the case of CP-even neutral states h and H , the mixing angle is naturally small in such away that h mimic the SM Higgs and H is a pure triplet. However, for some specific values of μ parameter (small μ), such mixing could be large and h becomes pure triplet and H pure doublet which mimic the SM Higgs.

The scalar sector has 8 parameters which we will take as λ , λ_i ($i = 1, \dots, 4$), μ , v_d and v_t . From those inputs, one can easily compute the physical masses and mixings [22]. We will perform a systematic scan over the eight parameters taking into account perturbative unitarity as well as vacuum stability constraints as given in [22].

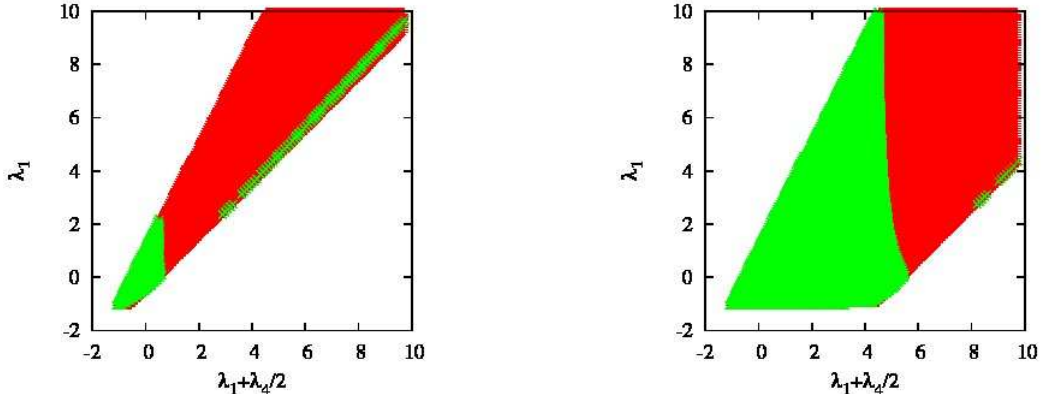


FIG. 3: (red) Allowed parameter space for λ_1 and λ_4 by theoretical constraints, (green) allowed parameter space for λ_1 and λ_4 taking into account $R_{\gamma\gamma} = 1.18 \pm 0.16$ at the 3- σ level. With $\lambda_3 = 2\lambda_2$, $-10 < \lambda_2 < 10$, $v_t = 1$ GeV and $\mu = 1$ GeV (left), $\mu = 8$ GeV (right).

A. Numerical results for HTM

If the Higgs boson h is fully dominated by the doublet component, as it will be the case in this presentation, the production cross section in HTM and in SM would be the same. $R_{V\gamma}$ defined in eq. (6) will reduce to the ratio of branching ratios.

The analytic expression for $h \rightarrow \gamma\gamma$ can be found in [22] which contains the additional contribution from H^\pm and $H^{\pm\pm}$. Like for $h \rightarrow \gamma\gamma$, the expression for $h \rightarrow Z\gamma$ in the HTM [19] can be derived from eq. (4) by adding adequate couplings of the Higgs to top quark, W boson, $H^{\pm\pm}$ and H^\pm in HTM. We remind the reader that in the SM, $h \rightarrow \gamma\gamma$ and $h \rightarrow Z\gamma$ are fully dominated by W gauge boson contributions. The contribution of those new charged particles H^\pm and $H^{\pm\pm}$ have an amplitude which can be constructive or destructive with the W depending on the SM Higgs coupling to a pair of H^\pm and $H^{\pm\pm}$ which are given by:

$$g_{h^0 H^{\pm\pm} H^\mp} \approx -\lambda_1 v_d \quad , \quad g_{h^0 H^\pm H^\pm} \approx -(\lambda_1 + \lambda_4/2)v_d \quad (11)$$

In the above formulas, we neglect the triplet vev and the mixing angles between doublet and triplet. It is clear from those couplings that $H^{\pm\pm}$ or H^\pm contributions are fixed respectively by λ_1 and $\lambda_1 + \lambda_4/2$ signs. In fact, H^\pm and $H^{\pm\pm}$ are constructive with the W contribution if $\lambda_1 < 0$ and $\lambda_1 + \lambda_4/2 < 0$.

In the following numerical studies, we will allow the doubly charged Higgs mass to be as low as 100 GeV. In fact, the actual limit from CMS on $H^{\pm\pm}$ decaying leptonically is of the order 450 GeV [23] for $H^{\pm\pm} \rightarrow e^\pm \mu^\pm$ channel. This limit can be reduced down to about 85 GeV if one takes into account the decay channels $H^{\pm\pm} \rightarrow W^\pm W^{\pm*}$ as well as the cascade decay $H^\pm \rightarrow H^\pm W^{\pm*}$ [12, 27].

Since the contribution of $H^{\pm\pm}$ and H^\pm depend on λ_1 and $\lambda_1 + \lambda_4/2$ signs. We can ask, what sign would prefer those quantities when taking into account all the theoretical constraints (perturbative and Boundedness from below (BFB) [22])? We perform a systematic scan over $-10 < \lambda_{1,2,4} < 10$ with $\lambda_3 = 2\lambda_2$ and $m_h = 126$ GeV, $v_t = \mu = 1$ GeV and the results are shown in Fig. (3). As one can see, the theoretical constraints prefer positive λ_1 and $\lambda_1 + \lambda_4/2$, only small area of parameter space with negative λ_1 and/or negative $\lambda_1 + \lambda_4/2$ is allowed. In this small area either $H^{\pm\pm}$ or H^\pm contributions or both of them are constructive with the W loops and therefore we would expect some enhancement in the diphoton rate without need for large $\lambda_{1,4}$. Note that we have also shown in Fig. (3) the constraint coming from the combination of ATLAS and CMS signal strength of the diphoton channel which we take roughly to be 1.18 ± 0.16 . Once this constraint is included at the 3- σ level, the allowed parameter space in λ_1, λ_4 plane shrink to the green area.

In Fig. (4), we illustrate the effect of λ_1 and $m_{H^{\pm\pm}}$ mass. It is clear that for negative λ_1 there is a small enhancement in the diphoton rate. Such diphoton enhancement can also take place for large and positive λ_1 with rather light $H^{\pm\pm}$ without violating the theoretical bounds. In fact, increasing λ_1 (for fixed λ_4 or $m_{H^{\pm\pm}}$) enhances $g_{h^0 H^{\pm\pm} H^\mp}$ and $g_{h^0 H^\pm H^\pm}$ couplings. For $\lambda_1 > 0$, the destructive interference between the SM loop contributions and those of H^\pm and $H^{\pm\pm}$ becomes then more and more pronounced. The leading HTM effect is mainly from the $H^{\pm\pm}$ contribution, the latter being enhanced with respect to H^\pm by a factor 4 due to the doubled electric charge, but also due to a smaller mass than the latter in some parts of the parameter space.

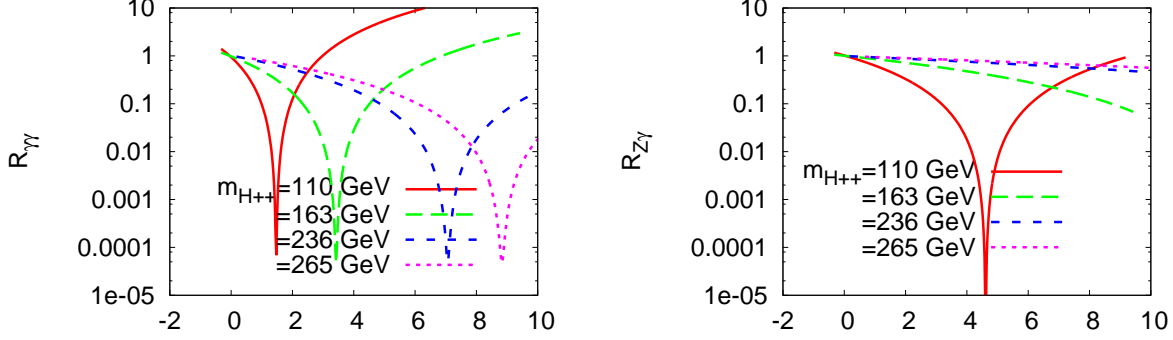


FIG. 4: Signal strength $R_{\gamma\gamma}$ (left) and the corresponding $R_{Z\gamma}$ (right) as a function of λ_1 for several values of $m_{H^{\pm\pm}}$ with $\mu = v_t = 1$ GeV and $\lambda_3 = 2\lambda_2 = 0.2$.

There exist thus necessarily values of λ_1 where the effect of the destructive interference is maximized leading to a tremendous reduction of $\Gamma(h \rightarrow \gamma\gamma)$. Since all the other decay channels remain SM-like, the same reduction occurs for $Br(h \rightarrow \gamma\gamma)$. The different dips seen in Fig. (4) are due to such a severe cancellation between SM loops and $H^{\pm\pm}$ and H^\pm loops, and they occur for λ_1 values within the allowed unitarity & BFB regions.

In the case of $h \rightarrow Z\gamma$, as far as the $H^{\pm\pm}$ contribution is concerned, the negative λ_1 is preferred in order to have an enhancement. The enhancement of $R_{Z\gamma}$ compared to the one of $R_{\gamma\gamma}$ will be suppressed by the coupling $g_{ZH^{\pm\pm}H^\mp}$ which is smaller than $g_{\gamma H^{\pm\pm}H^\mp}$. Moreover, in the HTM $g_{ZH^{\pm\pm}H^\mp}$ and $g_{ZH^\pm H^\mp}$ couplings have opposite signs, which imply a destructive interference between the dominant doubly charged $H^{\pm\pm}$ and a subdominant singly charged H^\pm contributions when $g_{hH^{\pm\pm}H^\mp}$ and $g_{hH^\pm H^\mp}$ couplings have same signs. In

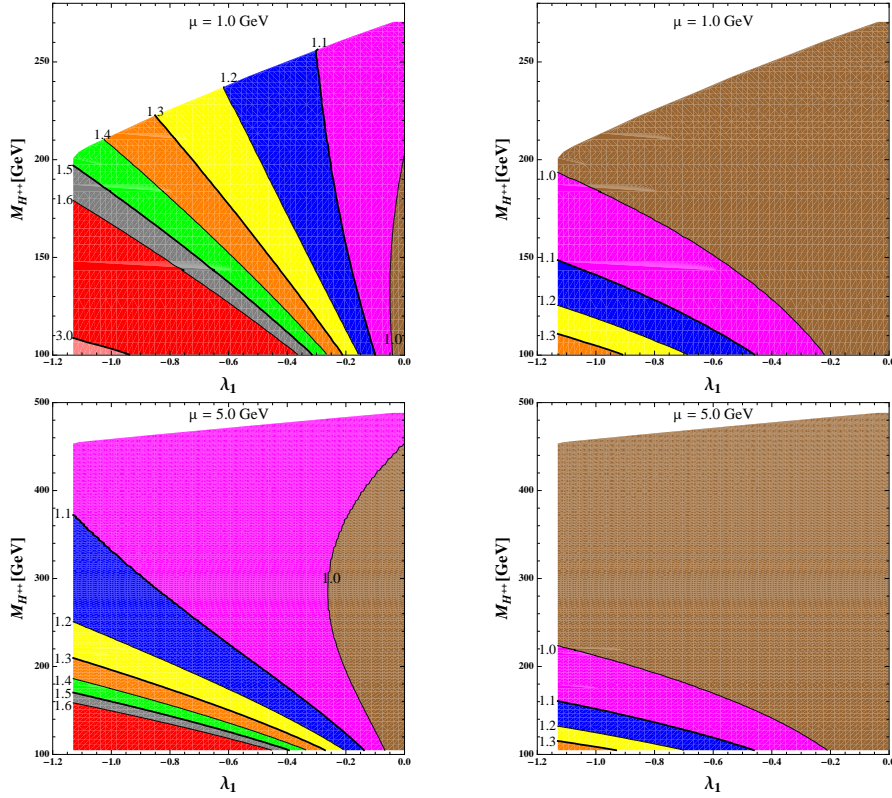


FIG. 5: Signal strength $R_{\gamma\gamma}$ (left) in $(\lambda_1, m_{H^{\pm\pm}})$ plane and the corresponding $R_{Z\gamma}$ (right). With $m_h = 126$ GeV, $v_t = 1$ GeV, $\lambda_4 = 2\lambda_2$, $\lambda_3 = 2\lambda_2$ and $-2 < \lambda_2 < 2$. Upper plots are for $\mu = 1$ GeV and lower plots for $\mu = 5$ GeV.

Fig.5, we illustrate $R_{\gamma\gamma}$ left panels and $R_{Z\gamma}$ right panels as a function of negative λ_1 and doubly charged Higgs mass. The effect of the $m_{H^{\pm\pm}}$ is clearly seen in those plots and can be summarized as:

- For $\mu = 1$ GeV, upper plots, one can see that $R_{\gamma\gamma} > 1.1$ (resp $R_{Z\gamma} > 1.1$) for $100 < m_{H^{\pm\pm}} < 250$ GeV (resp for $100 < m_{H^{\pm\pm}} < 150$ GeV). There is also a short brown area where $R_{\gamma\gamma} < 1$ where $H^{\pm\pm}$, H^\pm and W loops cancel each others. The brown area is bigger in the case of $R_{Z\gamma}$.
- For $\mu = 5$ GeV, lower plots, one can see that $R_{\gamma\gamma} > 1.1$ (resp $R_{Z\gamma} > 1.1$) for $100 < m_{H^{\pm\pm}} < 380$ GeV (resp for $100 < m_{H^{\pm\pm}} < 160$ GeV). Once more, the brown area correspond to $H^{\pm\pm}$, H^\pm and W loops cancel each others where $R_{\gamma\gamma} < 1$.

It is important to notice from Fig. (6)(right), that both correlation and anti-correlation between $R_{\gamma\gamma}$ and $R_{Z\gamma}$ are possible. For a fixed $R_{\gamma\gamma} > 1$, we can have 2 solutions for $R_{Z\gamma}$, one with enhanced $R_{Z\gamma} > 1$ rate and one with suppressed $R_{Z\gamma} < 1$ rate. On the other hand if $R_{\gamma\gamma} < 1$, we can have either $1 < R_{\gamma\gamma} < R_{Z\gamma}$ or $R_{Z\gamma} < R_{\gamma\gamma} < 1$. Note that an other situation which could happen, which is not favored by LHC measurements of diphoton channel, is a very suppressed $R_{\gamma\gamma} \approx 0$ while $R_{Z\gamma} \approx 0.4 - 0.6$.

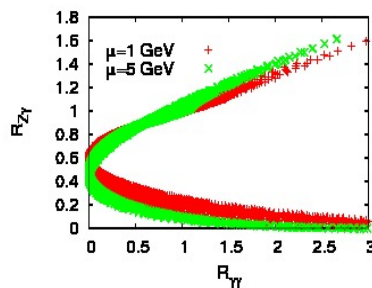


FIG. 6: Correlation between $R_{\gamma\gamma}$ and $R_{Z\gamma}$ with $\mu = 1$ and 5 GeV, $v_t = 1$ GeV, $m_h = 126$ GeV, $-10 < \lambda_{1,2,4} < 10$, $\lambda_3 = 2\lambda_2$. Allowed range for $R_{\gamma\gamma} \in [0, 3]$

V. CONCLUSIONS

We have shown that in the IDHM substantial diphoton excess is possible for light charged Higgs mass $m_{H^\pm} < 250$ GeV and negative λ_3 which will also leads to an enhancement of $h \rightarrow Z\gamma$ channel with $R_{\gamma\gamma}$ slightly larger than $R_{Z\gamma}$. For heavy charged Higgs mass $m_{H^\pm} \geq 300$ GeV and negative λ_3 one can still have $h \rightarrow \gamma\gamma$ enhancement but less than 10% .

In the case of type II seesaw model, taking into account all theoretical constraints on the Higgs potential such as perturbative unitarity and vacuum stability, we have shown that important diphoton excess is possible from light doubly charged Higgs loops together with negative $\lambda_1 \approx \mathcal{O}(1)$ or positive and large λ_1 . Such enhancement in the diphoton channel would rather be possible and more pronounced (more than 30%) if the doubly charged Higgs mass $m_{H^{\pm\pm}} \leq 400$ GeV. We have also illustrated that only a tiny region for negative λ_1 , compared to positive λ_1 , is allowed by perturbative unitarity and vacuum stability constraints. It has been also shown that in the HTM, one can have excess both in diphoton channel and $h \rightarrow Z\gamma$ channel. But it is also possible to have an enhancement in diphoton channel together with suppressed rate in $h \rightarrow Z\gamma$ with respect to SM. Both situations would be in favor of Higgs triplet model.

Acknowledgments

The author is grateful to the organizers for very stimulating workshop and would like to thanks Shynia Kanemura for the hospitality extended to him during his stay in Toyama. The author would like to thanks Maria Krawczyk and Jisuke Kubo for discussions. Large part of the work presented here is done in collaboration with R. Benbrik, M. Chabab, N. Gaur, G. Moultaqa and L. Rahili to whom I express my deep thanks for fruitful collaborations.

-
- [1] G. Aad *et al.* [ATLAS Collaboration], Phys. Lett. B **716**, 1 (2012) [arXiv:1207.7214 [hep-ex]].
- [2] S. Chatrchyan *et al.* [CMS Collaboration], Phys. Lett. B **716**, 30 (2012) [arXiv:1207.7235 [hep-ex]].
- [3] G. Aad *et al.* [ATLAS Collaboration], ATLAS note: ATLAS-CONF-2013-012
- [4] S. Chatrchyan *et al.* [CMS Collaboration], CMS-PAS-HIG-13-001
- [5] G. Aad *et al.* [ATLAS Collaboration], ATLAS note: ATLAS-CONF-2013-009 ; S. Chatrchyan *et al.* [CMS Collaboration], CMS-PAS-HIG-13-006
- [6] A. Arhrib, R. Benbrik and N. Gaur, Phys. Rev. D **85**, 095021 (2012) [arXiv:1201.2644 [hep-ph]].
- [7] B. Swiezewska and M. Krawczyk, arXiv:1212.4100 [hep-ph].
- [8] A. Arhrib, R. Benbrik, M. Chabab, G. Moulataka and L. Rahili, JHEP **1204**, 136 (2012) and arXiv:1202.6621 [hep-ph].
- [9] A. G. Akeroyd and S. Moretti, Phys. Rev. D **86**, 035015 (2012) [arXiv:1206.0535 [hep-ph]].
- [10] E. J. Chun, H. M. Lee and P. Sharma, JHEP **1211**, 106 (2012) [arXiv:1209.1303 [hep-ph]].
- [11] S. Kanemura and K. Yagyu, Phys. Rev. D **85**, 115009 (2012) [arXiv:1201.6287 [hep-ph]].
- [12] A. Melfo, M. Nemevsek, F. Nesti, G. Senjanovic and Y. Zhang, Phys. Rev. D **85**, 055018 (2012).
- [13] P. Fileviez Perez, H. H. Patel, M. J. Ramsey-Musolf and K. Wang, Phys. Rev. D **79**, 055024 (2009) [arXiv:0811.3957 [hep-ph]]. L. Wang and X. -F. Han, arXiv:1303.4490 [hep-ph].
- [14] See also talks by: M. Krawczyk, J. Kubo, K. Yagyu, E. J. Chun and M. Kikuchi in these proceedings.
- [15] C. -S. Chen, C. -Q. Geng, D. Huang and L. -H. Tsai, arXiv:1302.0502 [hep-ph].
- [16] C. -S. Chen, C. -Q. Geng, D. Huang and L. -H. Tsai, arXiv:1301.4694 [hep-ph].
- [17] P. S. B. Dev, D. K. Ghosh, N. Okada and I. Saha, JHEP **1303**, 150 (2013) [arXiv:1301.3453 [hep-ph]].
- [18] C. -W. Chiang and K. Yagyu, Phys. Rev. D **87**, 033003 (2013) [arXiv:1207.1065 [hep-ph]].
- [19] A. Arhrib, R. Benbrik, G. Moulataka and L. Rahili, work in progress
- [20] N. G. Deshpande and E. Ma, Phys. Rev. D **18**, 2574 (1978).
- [21] M. Spira, Fortsch. Phys. **46**, 203 (1998) [hep-ph/9705337]. J. F. Gunion, H. E. Haber, G. L. Kane and S. Dawson, Front. Phys. **80**, 1 (2000).
- [22] A. Arhrib, R. Benbrik, M. Chabab, G. Moulataka, M. C. Peyranere, L. Rahili and J. Ramadan, Phys. Rev. D **84**, 095005 (2011) [arXiv:1105.1925 [hep-ph]].
- [23] S. Chatrchyan *et al.* [CMS Collaboration], Eur. Phys. J. C **72**, 2189 (2012) [arXiv:1207.2666 [hep-ex]].
- [24] A. Arhrib, W. Hollik, S. Penaranda and M. Capdequi Peyranere, Phys. Lett. B **579**, 361 (2004).
- [25] J. F. Gunion and H. E. Haber, Phys. Rev. D **67**, 075019 (2003) [hep-ph/0207010].
- [26] T. P. Cheng and L. -F. Li, Phys. Rev. D **22**, 2860 (1980). J. Schechter and J. W. F. Valle, Phys. Rev. D **22**, 2227 (1980). R. N. Mohapatra and G. Senjanovic, Phys. Rev. D **23**, 165 (1981).
- [27] S. Kanemura, K. Yagyu and H. Yokoya, arXiv:1305.2383 [hep-ph].